IOP Publishing Journal of Optics
J. Opt. 19 (2017) 054004 (6pp) https://doi.org/10.1088/2040-8986/aa6901

Nonlinear behaviors in a PDE model for parity-time-symmetric lasers

Jianke Yang

Department of Mathematics and Statistics, University of Vermont, Burlington, VT 05401, United States of America

E-mail: jyang@math.uvm.edu

Received 11 February 2017, revised 13 March 2017
Accepted for publication 24 March 2017
Published 18 April 2017

Abstract

We propose a phenomenological time-dependent partial differential equation model to investigate the dynamical behaviors of certain parity-time ($\mathcal{PT}$) symmetric lasers during the nonlinear stage of their operations. This model incorporates physical effects such as the refractive index distribution, dispersion, material loss, nonlinear gain saturation and self-phase modulation. We show that when the loss is weak, multiple stable steady states and time-periodic states of light exist above the lasing threshold, rendering the laser multi-mode. However, when the loss is strong, only a single stable steady state of broken $\mathcal{PT}$ symmetry exists for a wide range of the gain amplitude, rendering the laser single-mode. These theoretical results corroborate the previous experimental results, and reveal the important role the loss plays in maintaining the single-mode operation of $\mathcal{PT}$ lasers.

Keywords: nonlinear optics, parity-time symmetry, laser model

(Some figures may appear in colour only in the online journal)

1. Introduction

Parity-time ($\mathcal{PT}$) symmetry was first introduced as a non-Hermitian generalization of quantum mechanics in 1998, where it was reported that a class of complex potentials possessing the $\mathcal{PT}$ symmetry could also feature all-real spectra [1]. This concept later spread to optics, where a judicious balancing of gain and loss constitutes a $\mathcal{PT}$-symmetric system [2–6]. Properties of $\mathcal{PT}$ systems have been extensively studied in the past ten years (see [7, 8] for reviews). More importantly, applications of $\mathcal{PT}$ symmetry have started to emerge [9–12]. Of particular interest is a $\mathcal{PT}$ microring laser [11, 12]. By intentionally introducing loss into the laser cavity, it was shown that these lasers are capable of single-mode operations. These operations were explained using a linear coupled-mode ordinary differential equation (ODE) model. However, it is well known that lasing is an inherent nonlinear process. In order to investigate the nonlinear stage of these $\mathcal{PT}$ lasers, certain nonlinear coupled-mode ODE models were used [13, 14]. But such ODE models did not account for the effects of refractive-index distributions, dispersion, nonlinear self-phase modulation, and sometimes nonlinear modal interactions. In [14], a steady-state *ab initio* laser theory was also employed, but a dynamic (time-dependent) model would be more desirable since only a dynamical model could address the question of stability of steady-state laser states.

The $\mathcal{PT}$ lasers of [11, 12] utilized microrings as laser cavities. It is also possible to realize $\mathcal{PT}$ lasers using traditional semiconductor cavities comprising twin stripes, one with gain and the other with loss [15, 16]. A study of nonlinear behaviors in such semiconductor $\mathcal{PT}$ lasers is also desirable.

In this article, we propose a phenomenological time-dependent partial differential equation (PDE) model to investigate the dynamical behavior of $\mathcal{PT}$ lasers during their nonlinear stage of operation. This model incorporates the physical effects such as the refractive index distribution, dispersion, spatially-modulated linear loss, spatially-modulated nonlinear saturable gain, and nonlinear self-phase modulation. Even though this PDE model is more elaborate than the previous coupled-mode ODE models, it is still simple enough for theoretical analysis. Using this model, we show that when the loss is weak, multiple stable steady states and time-periodic states of light exist above the lasing threshold, rendering the laser multi-mode. However, when the loss is

 © 2017 IOP Publishing Ltd Printed in the UK

strong, only a single stable steady state of broken $\mathcal{PT}$ symmetry exists for a wide range of the gain amplitude, rendering the laser single-mode. These theoretical results qualitatively agree with the experimental results in [11, 12], and they show that the loss plays a critical role in maintaining the single-mode operation of $\mathcal{PT}$ lasers.

2. A phenomenological PDE model

Lasing is a complicated process, and its accurate modeling is difficult or impossible. Thus, phenomenological laser modeling is often necessary [15]. For instance, one of the celebrated phenomenological models for mode-locked lasers is the Haus master equation [17], which played an important role in the theoretical understanding of passive mode-locked pulse lasers.

For $\mathcal{PT}$ lasers, the physical effects such as the spatial refractive index distribution, spatial material loss profile and nonlinear gain saturation are clearly very important. Another important physical effect is dispersion/diffraction, which has been included in the modeling of other semiconductor lasers [16]. In addition, we believe self-phase modulation also plays a significant role. With these factors in mind, we propose the following phenomenological PDE model

$$\mathrm{i}\Psi_t + \Psi_{xx} + V(x)\Psi + \sigma|\Psi|^2\Psi - \mathrm{i}\frac{G(x)}{1+|\Psi|^2}\Psi = 0, \quad (2.1)$$

where Ψ is a complex envelope function of the light's electromagnetic field, t and x are the time and space variables, $V(x) = n(x) + \mathrm{i}\Gamma(x)$ is the complex potential whose real part $n(x)$ describes the refractive-index distribution and the imaginary part $\Gamma(x)$ represents the linear (material) loss, σ is the coefficient of nonlinear self-phase modulation, $G(x)$ is the spatially-modulated linear gain, which is saturable at high intensities. All variables have been normalized.

This model is spatially one-dimensional (1D) for simplicity. It may be applied to potential semiconductor $\mathcal{PT}$ lasers with the cavity comprising twin stripes with respective gain and loss (under the mean field approximation along the light-propagation direction) [16]. The 1D model is also relevant to some 2D microring $\mathcal{PT}$ lasers (for instance in [12]) if the radiuses of the rings are relatively large so that the curvatures of the rings can be neglected.

In this 1D model, we consider two nearby regions with identical refractive-index and loss distributions, but the gain is applied only to the left region. This configuration resembles that in [12]. Corresponding to this configuration, we choose functions in the model (2.1) as

$$n(x) = n_0\,[f_1(x+x_0) + f_1(x-x_0)], \quad (2.2)$$

$$\Gamma(x) = \gamma\,[f_2(x+x_0) + f_2(x-x_0)], \quad (2.3)$$

$$G(x) = g f_3(x+x_0), \quad (2.4)$$

where $f_1(x), f_2(x), f_3(x)$ are spatial distributions of the refractive index, linear loss and gain in each region, n_0, γ and g are their peak values, and $-x_0$ and x_0 are the center positions of the two regions. For simplicity, we select f_1, f_2, f_3 to

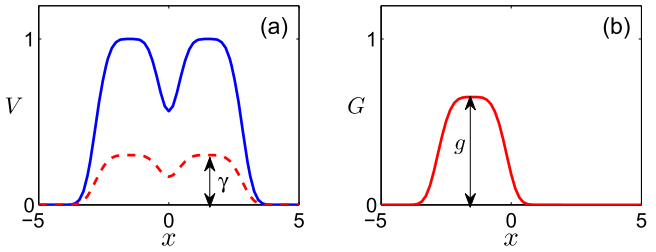

Figure 1. (a) Profiles of the refractive index distribution $n(x)$ (solid blue) and the linear loss function $\Gamma(x)$ (dashed red). (b) Profile of the gain function $G(x)$.

be the same super-Gaussian function

$$f_1(x) = f_2(x) = f_3(x) = \mathrm{e}^{-x^4/4}. \quad (2.5)$$

In addition, we select $n_0 = 1$ and $x_0 = 1.5$. Regarding the nonlinear coefficient σ, we set $\sigma = 0.5$, which is self-focusing nonlinearity. Then, the remaining free parameters in our model are the loss coefficient γ and the gain amplitude g. The resulting profiles of $n(x)$, $\Gamma(x)$ and $G(x)$ are displayed in figure 1. When $g = 2\gamma$, the effective linear potential $V(x) - \mathrm{i}G(x)$ is $\mathcal{PT}$-symmetric; thus the model (2.1) is $\mathcal{PT}$-symmetric in the linear regime. But due to gain saturation at higher amplitudes, the nonlinear model (2.1) is non-$\mathcal{PT}$-symmetric. When $g \neq 2\gamma$, this model is non-$\mathcal{PT}$-symmetric in both linear and nonlinear regimes.

Non-$\mathcal{PT}$ symmetry is an important feature of the nonlinear model (2.1) with gain saturation. Without gain saturation, this equation can be written as a nonlinear Schrödinger (NLS) equation with a complex linear potential. When this linear potential is $\mathcal{PT}$-symmetric, the underlying $\mathcal{PT}$-symmetric NLS equation has been thoroughly investigated for a wide variety of gain-loss profiles and spatial geometries [2, 8, 18, 19]. One common feature of those $\mathcal{PT}$-symmetric NLS equations is that their stationary localized modes (solitons) exist as continuous families, akin to conservative systems. In the presence of gain saturation, however, the nonlinear model (2.1) is non-$\mathcal{PT}$-symmetric. In this case, solitons exist only as isolated entities, as in typical dissipative systems [20]. The NLS equation with a linear but non-$\mathcal{PT}$-symmetric potential has also been investigated in [21], but the gain saturation was not considered there.

3. Solution analysis

Now, we investigate solution behaviors of the model (2.1) for a fixed loss coefficient γ and a tunable gain amplitude g. Soliton solutions are of the form

$$\Psi(x,t) = \mathrm{e}^{\mathrm{i}\mu t}\psi(x), \quad (3.1)$$

where $\psi(x)$ is a localized function solving

$$\psi_{xx} + V(x)\psi + \sigma|\psi|^2\psi - \mathrm{i}\frac{G(x)}{1+|\psi|^2}\psi = \mu\psi, \quad (3.2)$$

and μ is a real frequency parameter. Since equation (2.1) is non-$\mathcal{PT}$-symmetric, solitons exist only at isolated frequency values. We will compute these isolated solitons by the

squared operator method developed in [22], which yields the soliton profile $\psi(x)$ as well as the frequency value μ simultaneously.

To determine the linear stability of these solitons, we perturb them by normal modes as

$$\Psi(x, t) = \mathrm{e}^{\mathrm{i}\mu t}[\psi(x) + \tilde{\psi}(x)\mathrm{e}^{\lambda t} + \tilde{\phi}^*(x)\mathrm{e}^{\lambda^* t}], \tag{3.3}$$

where $|\tilde{\psi}|, |\tilde{\phi}| \ll |\psi|$. Substituting it into equation (2.1) and linearizing, we arrive at the eigenvalue problem

$$\mathcal{L}\begin{pmatrix}\tilde{\psi}\\ \tilde{\phi}\end{pmatrix} = \lambda\begin{pmatrix}\tilde{\psi}\\ \tilde{\phi}\end{pmatrix}, \tag{3.4}$$

where

$$\mathcal{L} = \begin{pmatrix}L_{11} & L_{12}\\ L_{12}^* & L_{11}^*\end{pmatrix}$$

is the linear-stability operator with entries

$$L_{11} = \mathrm{i}[\partial_{xx} - \mu + V(x) + 2\sigma|\psi|^2] + \frac{G}{(1+|\psi|^2)^2},$$

$$L_{12} = \psi^2\left(\mathrm{i}\sigma - \frac{G}{(1+|\psi|^2)^2}\right),$$

and λ is the eigenvalue. This eigenvalue problem can be computed by the Fourier collocation method (for the full spectrum) or the Newton-conjugate-gradient method (for individual discrete eigenvalues) [23]. If eigenvalues with positive real parts exist, the soliton is linearly unstable; otherwise it is linearly stable.

3.1. The case of lower loss

First we consider the lower-loss case, where we set $\gamma = 0.2$. In this case, lasing occurs (i.e., infinitesimal light starts to amplify) when $g > 2\gamma = 0.4$. Thus, at the lasing threshold $g = 2\gamma = 0.4$, the linear system is in $\mathcal{PT}$-symmetric state. Above this lasing threshold, we have found a number of soliton branches, which are displayed in figure 2. Two of these branches bifurcate off the zero amplitude at $g = 0.4$. On the higher-power branch, solitons have an approximately symmetric profile (see 'b' on the lower panel) and can be said to be in $\mathcal{PT}$-symmetric state; while on the lower-power branch, solitons have a slightly asymmetric profile (see 'a' on the lower panel). At g increases, the 'a' branch undergoes a fold bifurcation and disappears, while the 'b' branch persists. When $g > 0.56$, two additional soliton branches (the 'c, d' branches) appear through another fold bifurcation, and their powers have a non-zero minimum threshold. On their higher-power branch, solitons reside primarily in the gain region (see 'd' on the lower panel) and can be said to be in broken-$\mathcal{PT}$-symmetry state [13, 14]; while on the lower-power branch, solitons reside in both the gain and loss regions (see 'c' on the lower panel).

Linear stability of the soliton branches in figure 2 is also marked in the same figure. It is seen that the two soliton branches bifurcating from $g = 0.4$ are stable when g is close to 0.4, but lose stability when g is larger (the 'a' branch loses stability when $g > 0.60$, while the 'b' branch loses stability when $g > 0.70$). Both losses of stability are due to Hopf bifurcations, where a pair of complex linear-stability eigenvalues cross the imaginary axis. After the Hopf bifurcation, the solitons become unstable. Simultaneously, stable time-periodic bound states appear. Regarding the upper two branches, the 'c' branch is always unstable, while the 'd' branch is stable. To corroborate these results, linear-stability spectra for the four solitons in figure 2 (at points 'a, b, c, d' of the power curve) are displayed in the four panels of figure 3 respectively. These spectra show that the two solitons at points 'a, b' (with $g = 0.59$) and the soliton at point 'd' are linearly stable, because all eigenvalues lie on the left side of the complex plane (including the imaginary axis). But the soliton at point 'c' is unstable due to the presence of a real positive eigenvalue.

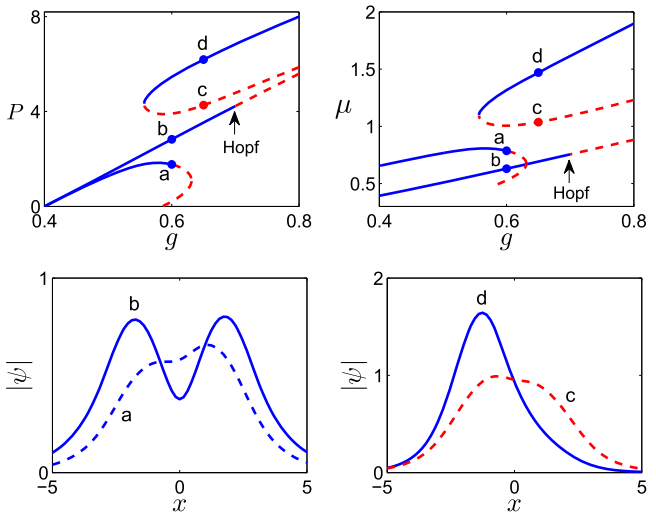

Figure 2. Soliton branches versus the gain coefficient g at the lower-loss value of $\gamma = 0.2$. Upper row: power and frequency branches (solid blue indicates stable solitons, and dashed red indicates unstable solitons). Lower row: soliton profiles at the marked points of the power/frequency branches. At points 'a, b', $g = 0.59$; at points 'c, d', $g = 0.65$.

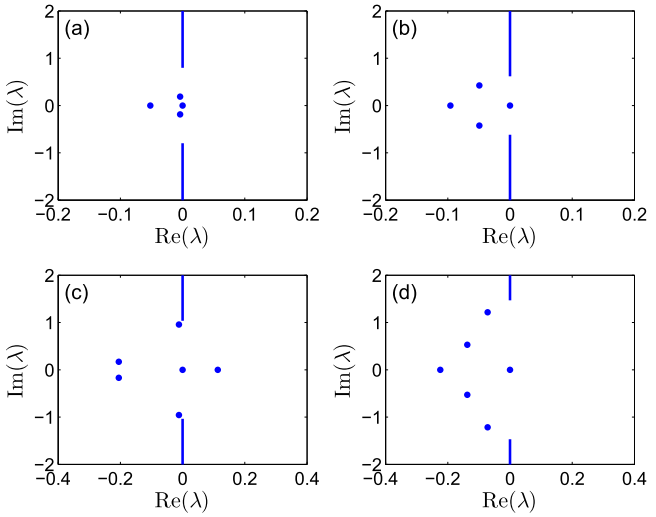

Figure 3. Linear-stability spectra for the four solitons shown in figure 2 respectively.

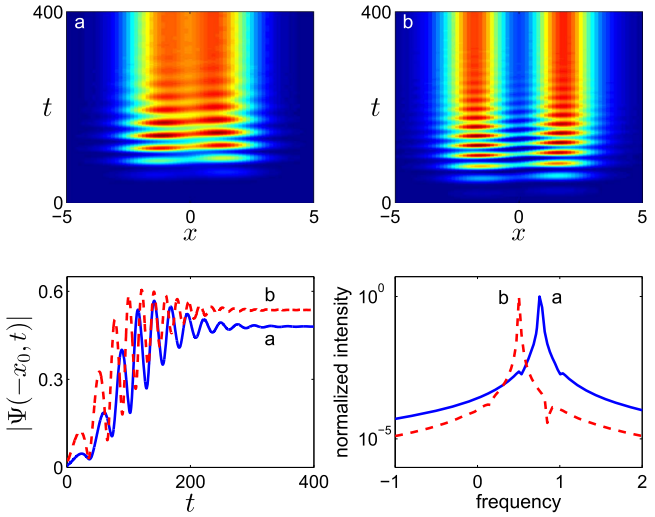

Figure 4. Evolutions of equation (2.1) for two different infinitesimal random-noise initial conditions when $\gamma = 0.2$ and $g = 0.5$. The lower panels show the amplitude evolutions and frequency spectra at the gain center $x = -1.5$.

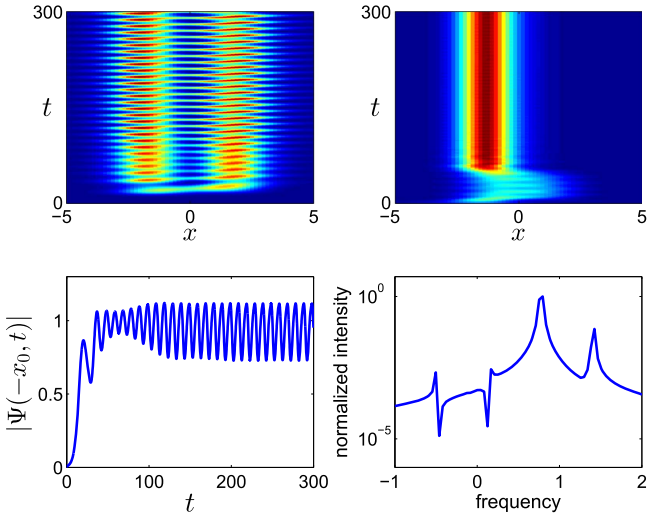

Figure 5. Evolutions of equation (2.1) for two different initial conditions when $\gamma = 0.2$ and $g = 0.72$ (the initial condition is infinitesimal in the upper left panel and has finite amplitude in the upper right panel). The lower panels show the amplitude evolution and frequency spectrum at the gain center $x = -1.5$ for the upper left panel.

Now we examine how light behaves in this lower-loss case. For this purpose, we consider two gain amplitudes, $g = 0.5$ and 0.72. When $g = 0.5$, figure 2 shows that there are two solitons which are both stable. Numerically, we have found that any infinitesimal initial condition would evolve toward one of these two stable solitons. To illustrate, numerical simulations of equation (2.1) for two different infinitesimal random-noise initial conditions are displayed in figure 4. The upper panels show that the two infinitesimal initial conditions are attracted toward different solitons. Amplitude evolutions and frequency spectra at the gain center $x = -x_0$, shown in the lower panels, confirm that the final states are solitons on the 'a' and 'b' branches of figure 2 respectively. Since these two solitons have different frequencies, this laser cavity can produce light of different frequencies and is thus not a single-mode laser.

At the higher gain amplitude $g = 0.72$ (which is above the Hopf bifurcation point of the 'b' branch in figure 2), the only stable soliton is on the 'd' branch. But a stable time-periodic bound state also exists due to this Hopf bifurcation (this time-periodic state can be directly computed by a numerical method developed in [24]). In this case, we have found numerically that all infinitesimal initial conditions are attracted toward that time-periodic bound state, see figure 5 (upper left panel). This temporal periodicity indicates that the output of light has multiple frequencies, as is evidenced in the lower right panel of figure 5. Thus, this laser is not single-mode either. For some finite-amplitude initial conditions, though, light can evolve toward the stable soliton on the 'd' branch, see the upper right panel of figure 5.

3.2. The case of higher loss

Next we consider the higher-loss case, where we set $\gamma = 0.5$. In this case, lasing occurs when $g > 0.66$. At this lasing threshold, the linear system is in broken $\mathcal{PT}$-symmetry state.

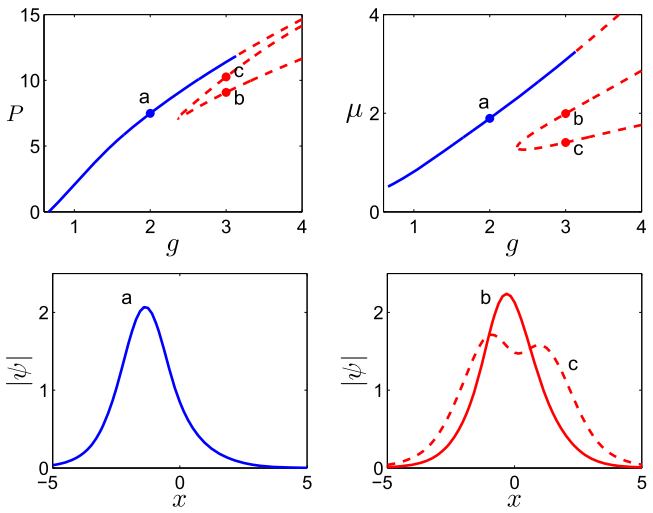

Figure 6. Soliton branches versus the gain coefficient g at the higher-loss value of $\gamma = 0.5$. Upper row: power and frequency branches (solid blue for stable solitons and dashed red for unstable solitons). Lower row: soliton profiles at the marked points of the power/frequency branches. At point 'a', $g = 2$; at points 'b, c', $g = 3$.

Above this threshold, soliton branches versus the gain amplitude g are displayed in figure 6. It is seen that a branch of stable solitons bifurcates from the zero amplitude at the lasing threshold, and it loses stability when $g > 3.1$. These solitons reside primarily in the gain region and thus have broken $\mathcal{PT}$-symmetry (see the lower left panel). Meanwhile, two branches of unstable solitons appear through a fold bifurcation when $g > 2.36$, and these solitons reside in both the gain and loss regions (see the lower right panel). To corroborate the stability results of these soliton branches, linear-stability spectra for the three solitons in figure 6 (at points 'a, b, c' of the power curve) are displayed in the three panels of figure 7 respectively. These spectra show that the

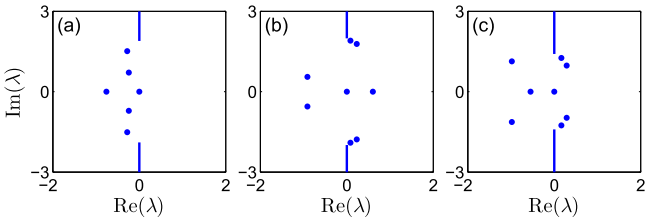

Figure 7. Linear-stability spectra for the three solitons shown in figure 6 respectively.

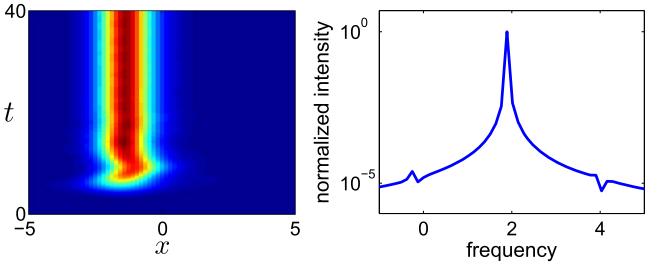

Figure 8. Evolution of equation (2.1) for an infinitesimal random-noise initial condition with $\gamma = 0.5$ and $g = 2$. The right panel shows the frequency spectrum at the gain center $x = -1.5$.

soliton at point 'a' is stable, but the solitons at points 'b, c' are unstable due to complex eigenvalues.

The striking feature in this case is that, over a wide gain interval of $0.66 < g < 3.1$, there is a single stable soliton, and no other stable coherent states (such as time-periodic states) exist. Our numerical simulations show that on this wide gain interval, all infinitesimal initial conditions evolve toward this single stable soliton (see figure 8), thus the laser is in single-mode operation.

By comparing the lower-loss operation in figures 2–5 and higher-loss operation in figures 6–8, we see that when the loss is weak, multiple stable solitons and time-periodic bound states exist above the lasing threshold, rendering the laser multi-mode. However, a strong loss can eliminate those multiple stable solitons and time-periodic states, leaving the system with a single stable soliton of broken $\mathcal{PT}$ symmetry and thus rendering the laser single-mode. These results qualitatively agree with the experimental results in [11, 12], and they reveal that the loss is instrumental in maintaining the single-mode operation of $\mathcal{PT}$ lasers.

4. Comparison with an ODE model

Some of the solution behaviors in the PDE model for the configuration of figure 1 can be understood from a simpler coupled-mode ODE model,

$$\frac{d\Phi_1}{dt} = -\alpha\Phi_1 + \frac{\beta}{1+|\Phi_1|^2}\Phi_1 + i\Phi_2, \tag{4.1}$$

$$\frac{d\Phi_2}{dt} = -\alpha\Phi_2 + i\Phi_1, \tag{4.2}$$

where Φ_1 and Φ_2 are the amplitudes of the supermodes in the gain (left) and loss (right) regions of the laser cavity

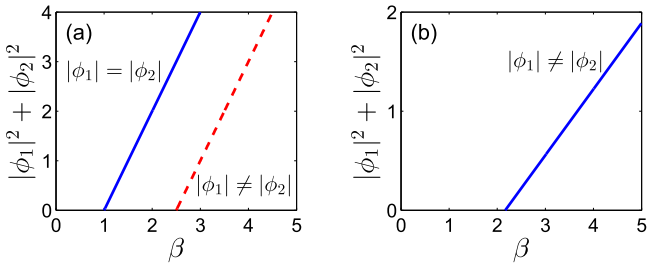

Figure 9. Power curves of steady states versus gain parameter β in the ODE model. (a) $\alpha = 0.5$ (lower loss); (b) $\alpha = 1.5$ (higher loss). Solid blue: stable states; dashed red: unstable states.

respectively, α is the linear material loss in both regions, and β is the linear growth rate of the saturable gain. The parameter values are normalized with respect to the coupling constant between the gain and loss regions. Similar but different ODE models have been used in [13, 14] to study various $\mathcal{PT}$-laser configurations.

Steady states of the above ODE model are of the form $\Phi_{1,2}(t) = e^{i\omega t}\phi_{1,2}$, where ω is a real frequency parameter, and ϕ_1, ϕ_2 are amplitude constants. Substituting this steady state into the ODE model, we find the following solutions,

$$(1)\ \omega = \pm\sqrt{1-\alpha^2}, \quad |\phi_1| = |\phi_2| = \sqrt{\beta/(2\alpha) - 1}\,; \tag{4.3}$$

$$(2)\ \omega = 0, \quad |\phi_1| = \sqrt{\beta/(\alpha + 1/\alpha) - 1}, \quad |\phi_2| = |\phi_1|/\alpha. \tag{4.4}$$

The two solutions (4.3) exist only when the loss is weak ($\alpha < 1$). They have identical amplitudes but different frequencies. In each solution, the modal amplitudes in the gain and loss regions are the same ($|\phi_1| = |\phi_2|$), and are thus in $\mathcal{PT}$-symmetric state. They bifurcate out from the zero amplitude at the lasing threshold $\beta = 2\alpha$, where the linear counterpart of the ODE model is $\mathcal{PT}$-symmetric. The other solution (4.4) exists for all loss values of α. In this solution, the modal amplitudes in the gain and loss regions are different, and are thus in broken-$\mathcal{PT}$-symmetry state. This solution bifurcates out from the zero amplitude at $\beta = \alpha + 1/\alpha$. To illustrate these solutions, we choose two loss values of $\alpha = 0.5$ (lower loss) and $\alpha = 1.5$ (higher loss), where the power values $|\phi_1|^2 + |\phi_2|^2$ of these solution branches versus the gain parameter β are displayed in figures 9(a), (b) respectively. Linear stability of these steady states has also been determined and marked on the figure. At lower loss, the two $\mathcal{PT}$-symmetric solutions (4.3) are both stable, rendering the laser multi-mode; and the broken-$\mathcal{PT}$-symmetry solution is unstable (see figure 9(a)). Our numerics shows that these two stable solutions (4.3) attract all infinitesimal initial conditions. At higher loss (see figure 9(b)), the sole broken-$\mathcal{PT}$-symmetry solution (4.4) is stable and attracts all infinitesimal initial conditions.

When comparing these ODE-model results with those PDE ones, we can see that at lower loss, the solid blue branch of two $\mathcal{PT}$-symmetric steady states in figure 9(a) is the counterpart of the two solid blue branches bifurcating

from $g = 0.4$ in figure 2 (upper left panel), and the dashed red branch of broken-$\mathcal{PT}$-symmetry states in figure 9(a) is the counterpart of the dashed red branch bifurcating from the zero power (at $g \approx 0.58$) in figure 2. At higher loss, the solid blue branch of broken-$\mathcal{PT}$-symmetry states in figure 9(b) is the counterpart of the solid blue branch bifurcating from the zero power in figure 6. Notice that at lower powers, solitons and their stability behaviors in the PDE model agree with their ODE counterparts. However, at higher powers, the PDE and ODE results show large differences. In particular, the ODE model fails to predict the new soliton branches from fold bifurcations at high powers, the Hopf bifurcations of soliton branches, and time-periodic bound states after Hopf bifurcations. The reason is that this ODE model implicitly assumes a fixed supermode profile in each of the gain and loss regions (only their amplitudes $\Phi_{1,2}$ are allowed to change with time). This assumption is reasonable for the PDE solutions at low powers, where the solutions are close to linear modes. However, at higher powers, the field profiles of PDE solutions will differ significantly from linear modes due to nonlinear self-focusing and other physical effects. In addition, the field profiles of PDE solutions can also oscillate with time (such as in time-periodic bound states, see figure 5), where multiple frequencies (modes) are mixed. In such cases, the ODE model cannot be expected to give good predictions, and a dynamic PDE model will become necessary, as is done in this article.

5. Summary

In summary, we have proposed a phenomenological time-dependent PDE model to investigate the dynamical behavior of certain $\mathcal{PT}$ lasers during the nonlinear stage of their operations. We have shown that when the loss is weak, multiple stable steady states and time-periodic states of light exist above the lasing threshold, rendering the laser multi-mode. However, when the loss is strong, only a single stable steady state of broken $\mathcal{PT}$ symmetry exists for a wide range of the gain amplitude, rendering the laser single-mode. Our results indicate that a significant amount of material loss is important for rendering the single-mode operation of $\mathcal{PT}$ lasers. These results qualitatively agree with the experimental results on $\mathcal{PT}$ lasers, which suggests that this PDE model may be useful for their theoretical predictions.

Acknowledgments

This material is based upon work supported by the Air Force Office of Scientific Research under award number FA9550-12-1-0244, and the National Science Foundation under award numbers DMS-1311730 and DMS-1616122.

References

[1] Bender C M and Boettcher S 1998 Real spectra in non-Hermitian Hamiltonians having $\mathcal{PT}$ symmetry *Phys. Rev. Lett.* **80** 5243
[2] Musslimani Z H, Makris K G, El-Ganainy R and Christodoulides D N 2008 Optical solitons in $\mathcal{PT}$-periodic potentials *Phys. Rev. Lett.* **100** 030402
[3] Rüter C E, Makris K G, El-Ganainy R, Christodoulides D N, Segev M and Kip D 2010 Observation of parity-time symmetry in optics *Nat. Phys.* **6** 192–5
[4] Driben R and Malomed B A 2011 Stability of solitons in parity-time-symmetric couplers *Opt. Lett.* **36** 4323
[5] Regensburger A, Bersch C, Miri M A, Onishchukov G, Christodoulides D N and Peschel U 2012 Parity-time synthetic photonic lattices *Nature* **488** 167–71
[6] Peng B, Özdemir S, Lei F, Monifi F, Gianfreda M, Long G, Fan S, Nori F, Bender C M and Yang L 2014 Parity-time-symmetric whispering-gallery microcavities *Nat. Phys.* **10** 394
[7] Suchkov S V, Sukhorukov A A, Huang J, Dmitriev S V, Lee C and Kivshar Y S 2016 Nonlinear switching and solitons in $\mathcal{PT}$-symmetric photonic systems *Laser Photon. Rev.* **10** 177
[8] Konotop V V, Yang J and Zezyulin D A 2016 Nonlinear waves in $\mathcal{PT}$-symmetric systems *Rev. Mod. Phys.* **88** 035002
[9] Longhi S 2010 $\mathcal{PT}$-symmetric laser absorber *Phys. Rev.* A **82** 031801
[10] Feng L, Xu Y L, Fegadolli W S, Lu M H, Oliveira J E B, Almeida V R, Chen Y F and Scherer A 2013 Experimental demonstration of a unidirectional reflectionless parity-time metamaterial at optical frequencies *Nat. Mater.* **12** 108
[11] Feng L, Wong Z J, Ma R, Wang Y and Zhang X 2014 Single-mode laser by parity-time symmetry breaking *Science* **346** 972–5
[12] Hodaei H, Miri M-A, Heinrich M, Christodoulides D N and Khajavikhan M 2014 Parity-time-symmetric microring lasers *Science* **346** 975–8
[13] Hassan A U, Hodaei H, Miri M, Khajavikhan M and Christodoulides D N 2015 Nonlinear reversal of PT symmetric phase transition in a system of coupled semiconductor micro-ring resonators *Phys. Rev.* A **92** 063807
[14] Ge L and El-Ganainy R 2016 Nonlinear modal interactions in parity-time (PT) symmetric lasers *Sci. Rep.* **6** 24889
[15] Agrawal G P and Dutta N K 1986 *Long-Wavelength Semiconductor Lasers* (New York: Van Nostrand-Reinhold)
[16] Miinkel M, Kaiser F and Hess O 1996 Spatio-temporal dynamics of multi-stripe semiconductor lasers with delayed optical feedback *Phys. Lett.* A **222** 67–75
[17] Haus H A 2000 Mode-locking of lasers *IEEE J. Sel. Top. Quantum Electron.* **6** 1173–85
[18] Barashenkov I V, Zezyulin D A and Konotop V V 2016 Jamming anomaly in $\mathcal{PT}$-symmetric systems *New J. Phys.* **18** 075015
[19] Zezyulin D A and Konotop V V 2016 Nonlinear currents in a ring-shaped waveguide with balanced gain and dissipation *Phys. Rev.* A **94** 043853
[20] Akhmediev N and Ankiewicz A (ed) 2005 *Dissipative Solitons* (Berlin: Springer)
[21] Zezyulin D A, Kartashov Y V and Konotop V V 2011 Solitons in a medium with linear dissipation and localized gain *Opt. Lett.* **36** 1200
[22] Yang J and Lakoba T I 2007 Universally-convergent squared-operator iteration methods for solitary waves in general nonlinear wave equations *Stud. Appl. Math.* **118** 153–97
[23] Yang J 2010 *Nonlinear Waves in Integrable and Nonintegrable Systems* (Philadelphia, PA: SIAM)
[24] Yang J 2015 A numerical method for computing time-periodic solutions in dissipative wave systems *Stud. Appl. Math.* **134** 420–55